frontiers | Frontiers in Materials

TYPE Original Research
PUBLISHED 05 November 2024
DOI 10.3389/fmats.2024.1490273

OPEN ACCESS

EDITED BY
Azra Kocaarslan,
Karlsruhe Institute of Technology (KIT), Germany

REVIEWED BY
Huseyin Kiliclar,
Istanbul Technical University, Türkiye
Derya Unlu,
Bursa Technical University, Türkiye

*CORRESPONDENCE
Sermet Koyuncu,
skoyuncu@comu.edu.tr

RECEIVED 02 September 2024
ACCEPTED 24 October 2024
PUBLISHED 05 November 2024

CITATION
Tohtayeva J, Altınışık S, Akgün M, Uğur Nigiz F and Koyuncu S (2024) Solar light driven photochromic membranes with viologen additives in PVDF/PVP matrix.
Front. Mater. 11:1490273.
doi: 10.3389/fmats.2024.1490273

Solar light driven photochromic membranes with viologen additives in PVDF/PVP matrix

Jahan Tohtayeva[1], Sinem Altınışık[1,2], Mert Akgün[2], Filiz Uğur Nigiz[1,2] and Sermet Koyuncu[1,2]*

[1]Department of Energy Resources and Management, Çanakkale Onsekiz Mart University, Çanakkale, Türkiye, [2]Department of Chemical Engineering, Çanakkale Onsekiz Mart University, Çanakkale, Türkiye

This study explores the synthesis and characterization of photochromic Polyvinylidenefluoride/Polyvinylpyrrolidone (PVDF/PVP)-based membranes, prepared through an *in situ* thiol-ene click reaction by incorporating viologen derivatives with different counter ions. Viologens are well-known for their light-sensitive properties and ability to change color, making them useful in various optoelectronic applications. The membranes developed in this study exhibit significant improvements in their interactions with light as a result of improved morphology and enhanced ionic conductivity (≈4×10^{-4} S cm^{-1}) with higher porosity (Ra: 11.26–33.76 nm) compared to conventionally prepared membranes. These membranes show the ability to block almost all ultraviolet (UV) and a 90% of visible light after irradiation. Thanks to these properties, the membranes undergo visible color changes when exposed to sunlight, making them suitable for photochromic and thermochromic applications. The findings of this study could contribute to the development of innovative coating materials that enhance energy efficiency, potentially being applied to buildings, automotive windows, and other surfaces.

KEYWORDS

viologen, thiol-ene click reaction, photochromic membrane, energy saving, coatings

1 Introduction

Photochromic materials, which undergo reversible photoisomerization from a colorless to a colorful state in the presence of ultraviolet (UV) or visible light spectrum, have the unusual capacity to revert to their initial state in the absence of light via visible (Vis) light or thermal relaxation (Tian and Zhang, 2016). These materials are widely used in aesthetical decorations, photography, memory, switches, display, photo mechanics, protection as camouflage, and photometry fields and these applications received high interest due to their actual or future use potential (Wang et al., 2010; Zhang et al., 2013; Shi et al., 2019; Ru et al., 2021). This inherent reversibility highlights their prospective uses in photoelectric disciplines, specifically in the creation of smart materials such as energy-saving membranes. Photochromic materials have been extensively studied and can be split into two major groups: organic materials (e.g., diarylethene, azobenzene, and spiropyran)

(Javed et al., 2016; Tsuruoka et al., 2016; Kaiser et al., 2017; Wu et al., 2017) and inorganic (e.g., rare earth complex-es, metal halides, and transition metal oxides) (Duncan et al., 1970; Ju et al., 2013; Chen et al., 2015a; Chen et al., 2015b; Du et al., 2024). In general, inorganic compounds offer great thermal stability, high strength, and diverse coordination chemistry, whereas organic compounds are diverse and simple to adjust or process (Tang et al., 2022). On the other hand, viologens represent an important class of photochromic materials (Kan et al., 2017). Due to its electron-accepting characteristics, viologen has been extensively studied in also electrochromics (Pathak and Moon, 2022), photovoltaics (Sharma et al., 2003), battery (Sen et al., 2013) and supercapacitor (Ambrose et al., 2023) applications since Michaelis discovered it in 1932 (Michaelis, 1935). One of the most remarkable aspects of viologen is its photoinduced color modification, which occurs when electrons from the counter anion are transferred to the viologen dication via a photoinduced effect (Xu et al., 2007).

Polyvinylidene fluoride (PVDF) stands as a semi-crystalline polymer distinguished by its semi-fluorinated nature, comprising CH_2 and CF_2 bonds (Dallaev et al., 2022). Notably, PVDF exhibits superior mechanical strength when compared to polytetrafluoroethylene (Teflon) (Rajeevan et al., 2021). PVDF membrane has been intensively researched as a viable candidate to use in membrane contactors and membrane distillation due to its great mechanical strength, outstanding thermal stability, and excellent chemical resistance (Liu et al., 2011). The polymer boasts commendable thermal stability, chemical resistance to ultraviolet and higher energy radiation, and resistance to a wide spectrum of chemicals and solvents, as documented by Lee et al. (2019). Subsequently, the purpose of using PVDF in this research is to subject PVDF-doped membranes to high-energy radiation under UV light for enhanced analysis. Besides, Polyvinylpyrrolidone (PVP) is also explored in photochromic applications due to their ability to form stable polymer matrices that can host photoactive compounds (Kozlov et al., 2019). In such systems, PVP's hydrophilic nature aids in the uniform dispersion of photochromic molecules, enabling efficient light-induced color changes. This makes PVP membranes suitable for use in smart coatings, optical devices, and UV-sensitive materials, where their transparency and flexibility further enhance performance (Li C. et al., 2020; Li Z. et al., 2020; Kayani et al., 2021).

The thiol-ene click reaction is characterized by the specific and efficient interaction between a compound containing a thiol group and another containing an alkene group. This reaction proceeds through a radical-mediated mechanism, which is initiated by light or radiation (Hoyle and Bowman, 2010). Due to these characteristics, thiol-ene systems hold significant value in polymer science. Notably, their ability to react effectively at low temperatures and across a broad range of solubilities makes them particularly suitable for life sciences and biomedical applications (Davis and Carter, 2015). In polymerization processes, the thiol-ene click reaction facilitates the synthesis of high molecular weight polymers whose adaptable structures permit the incorporation of various functional groups into the polymer chain (Davis and Carter, 2014). Additionally, this method is crucial for creating cross-linked network structures, which enhance the mechanical and chemical properties of the polymers. Ultimately, these cross-linked polymers are employed in membrane technologies, notably in applications such as water purification and gas separation (Martin et al., 2016). Thiol-ene-based membranes are distinguished by their high selectivity and permeability, as well as their chemical stability and mechanical robustness, thereby contributing to sustainable environmental solutions (Davis et al., 2011). Therefore, the thiol-ene click reaction, known for its high efficiency and selectivity under UV radiation, is employed to functionalize PVDF-doped membranes. This combination allows for the precise modification of PVDF surfaces, enhancing their performance in targeted applications.

Herein, this study is to demonstrate the photochromic properties of PVDF/PVP-based membranes prepared by doping with cross-linkable viologens containing different counter anions ($-BF_4^-$, $-ClO_4^-$ or $-PF_6^-$) to adjust the ionic conductivity of the membranes (Figure 1). The research aims to refine ion exchange properties and morphological characteristics of the membrane through fundamental characterization measurements. Additionally, examining the absorbance/transmittance changes under 366 nm and solar light revealed that the membrane almost completely blocked all UV and visible regions after light irradiation. Color changes under sunlight indicate a great potential of M-ALV-X membranes for use as energy-saving coating materials. This study provides essential results to guide future research in developing cost-effective, high-performance alternative membranes, thereby supporting the advancement of materials science and enhancing smart energy-saving technologies.

2 Results and discussion

First, 1,1′-diallyl-4,4′-bipyridinium bromide (ALV-Br) was prepared from previously published procedures (Koyuncu and Ayaşlıgil, 2023). Afterward, ALV-X molecules were prepared using different salts using the ion exchange method (See Supplementary Scheme S1). ALV-X structures were characterized by FT-IR, ^{1}H-NMR, and XRD analysis (See Supplementary Figures S1–S5) The structural characterization of M_ALV-X-based membranes, which were prepared with a thickness of approximately 120 μm, was performed using the FT-IR technique (Figure 2A). The presence of the PVP polymer in the membranes enhances their hydrophilicity, notably reflected in the O-H peak observed at about 3,300 cm^{-1} in the pure membrane. When ALV-X was added to the membrane, the water retention capacity of the membranes decreased due to more effective cross-linking under UV light and a reduction in the O-H bond transition at 3,300 cm^{-1}. A symmetric C-H vibration peak is observed around 2,900 cm^{-1}. The absorption peak at 1,410 cm^{-1} is attributed to $-CH_2$ vibrations, with its intensity diminishing due to the influence of viologen. At 1,185 cm^{-1}, the C-C bond in PVDF is detected. The peaks at 878 and 840 cm^{-1} are associated with the asymmetric C-C-C stretching and C-F stretching vibrations of PVDF, respectively. Besides, compared to the pristine PVDF/PVP membrane, peaks corresponding to the C=O bonds of the PETMP cross-linker at 1,780 cm^{-1} and C-S bonds at 960 cm^{-1} are observed. Additionally, peaks associated with the viologen moieties incorporated into the structure are noted around 1,620 cm^{-1} and 1,170 cm^{-1}. These observed specific peaks indicate that the ALV-X photoactive

10.3389/fmats.2024.1490273

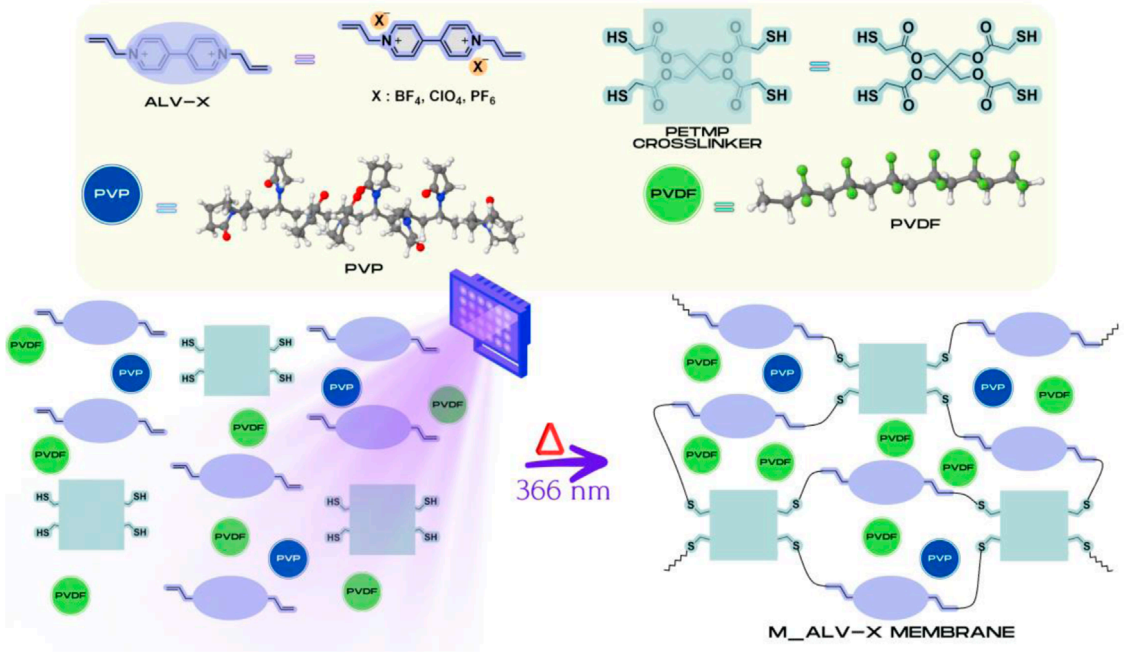

FIGURE 1
Preparation of PVDF/ALV-X-based membranes.

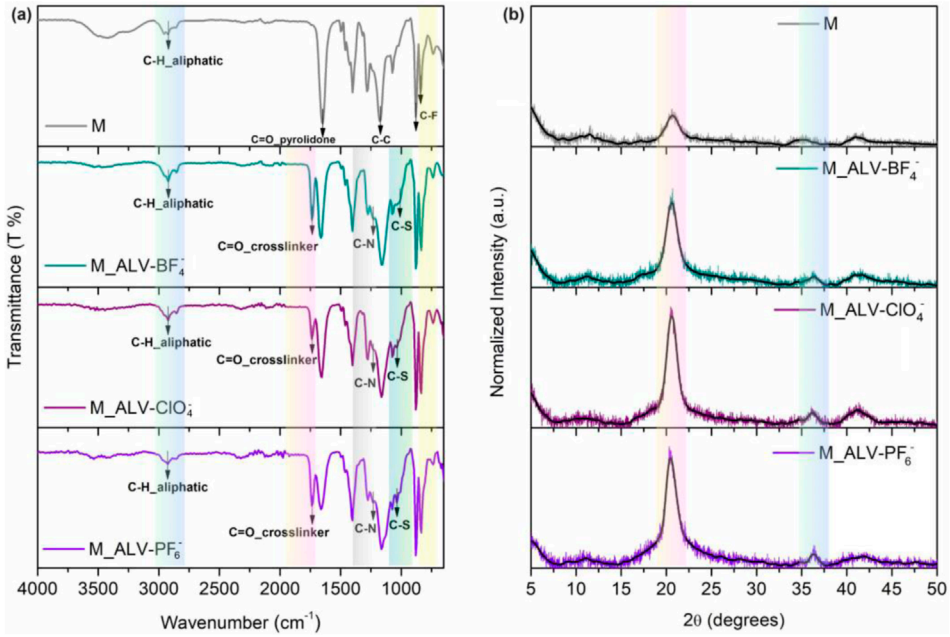

FIGURE 2
FTIR analysis of pristine PVDF/PVP membrane (M) and viologen doped PVDF/PVP (M-ALV-X) **(A)** and XRD pat-tern of pristine PVDF/PVP membrane (M) and viologen doped PVDF/PVP (M-ALV-X) **(B)**.

structures have been successfully incorporated into the PVDF membrane structure. The crystallinity of the membranes was investigated by XRD measurements. Figure 2B shows the XRD patterns obtained for PVDF-PVP membranes containing different viologens. The general features of the observed patterns prove the existence of a semi-crystalline structure. The XRD pattern of PVDF-PVP membranes showed the amorphous nature of the sample with a peak around 2θ = 20.41. The crystal intensity

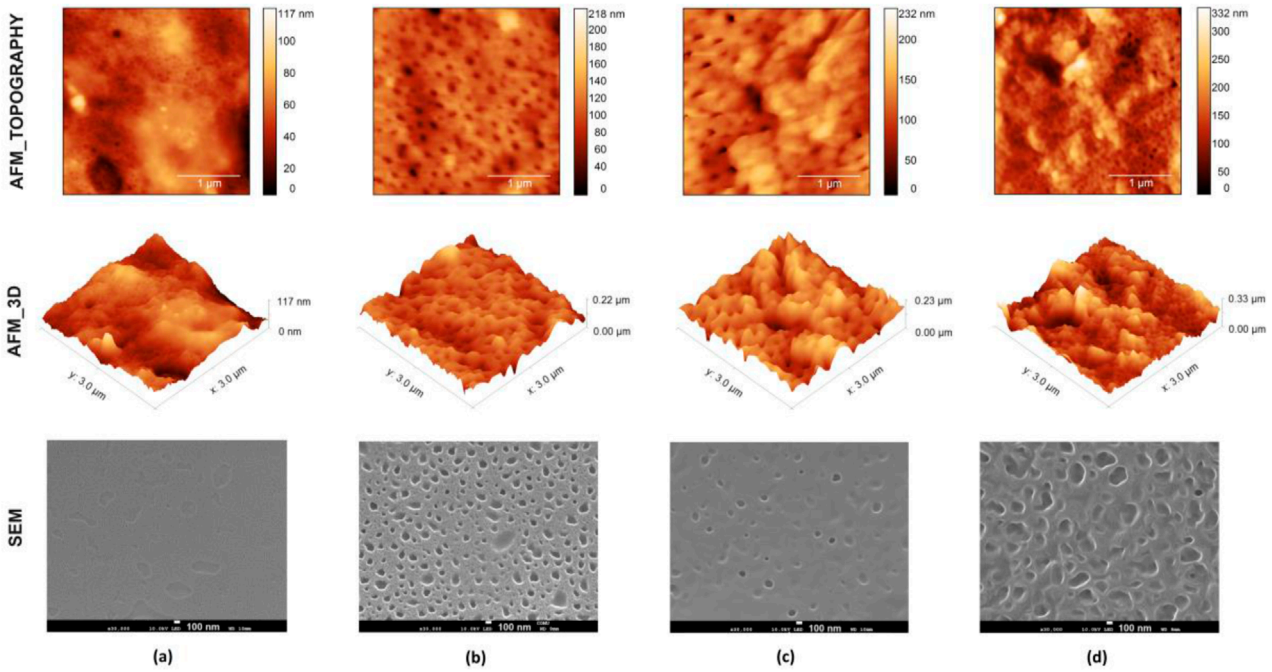

FIGURE 3
AFM and SEM images of pristine PVDF/PVP-M **(A)** and M_ALV-BF_4^- **(B)**, M_ALV-ClO_4^- **(C)**, M_ALV-PF_6^- **(D)** membranes.

TABLE 1 Ionic exchange capacity of M_ALV-X membranes.

Membrane	Swelling degree (%)	Water absorption (%)	IEC (mmol g^{-1})
PVDF/PVP	8.0	19.5	0.59
M_ALV-BF_4^-	8.1	19.9	1.32
M_ALV-ClO_4^-	8.2	19.7	1.18
M_ALV-PF_6^-	8.2	19.6	0.86

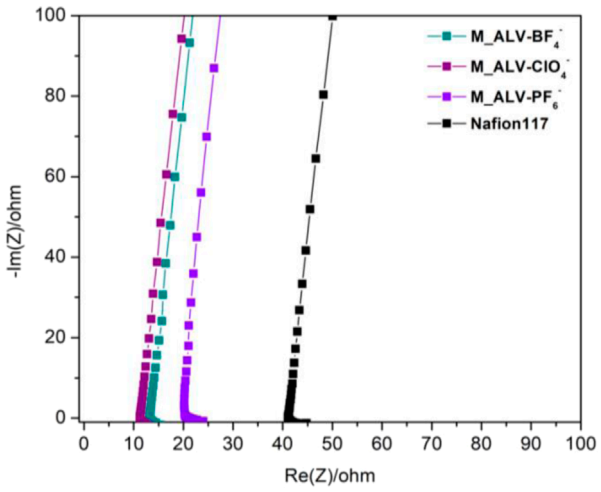

FIGURE 4
EIS Nyquist plots of Nafion 117 and M_ALV-X membranes.

increased with the addition of different viologen salts in the XRD pattern of the PVDF-PVP membranes (Bhatti et al., 2013). The relatively more crystalline behavior of the M_ALV-X polymeric membrane can be attributed to the crystalline properties of the pristine ALV-X additive (See Supplementary Figure S5).

The AFM image of the pristine PVDF/PVP membrane shows a very smooth surface (Ra: 4.32 nm). After the *in situ* cross-linking reaction of ALV-X molecules within the membrane, an increase in surface roughness and the formation of pinholes are observed (Figure 3). Notably, the M_ALV-BF_4^- membrane exhibits a more uniformly distributed hollow surface compared to the other membranes. This uniformity can positively influence the photochromic performance by enhancing ionic mobility under light exposure. Conversely, due to the larger diameter of the PF_6^- counterion, the roughness value (R_a) of the M_ALV-PF_6^- membrane, measured at 33.76 nm, is higher than that of the other membranes (11.26 nm for M_ALV-BF_4^- and 14.35 nm for M_ALV-ClO_4^-). SEM-EDX measurements were performed on the membranes prepared to support AFM measurements, determining both the chemical composition and surface properties. Upon examining the SEM images, it was observed that the addition of viologen derivatives to the PVDF/PVP membrane resulted in the formation of rougher surfaces, consistent with the AFM images. Additionally, SEM images revealed some cracks and de-formations on the PVDF/PVP

TABLE 2 Ion transport properties of Nafion 117 and M_ALV-X membranes.

Membrane	Thickness (μm)	Resistance (ohm)	Conductivity (S cm^{-1})
M_ALV-BF_4^-	120.1	12.3	3.11×10^{-4}
M_ALV-ClO_4^-	121.5	10.4	3.72×10^{-4}
M_ALV-PF_6^-	119.8	19.8	1.92×10^{-4}
Nafion 117	120.6	40.2	9.55×10^{-5}

membrane surface, which were attributed to the crystalline structure of the material. Furthermore, while a more uniform porous structure distribution was observed in the M_ALV-BF_4^- and M_ALV-PF_6^- membranes, it was noted that the pore diameters increased up to 400–500 nm due to the larger ion diameter of M_ALV-PF_6^-. This porous structure enhances the surface area, providing an advantage for various applications (Sun et al., 2016). On the other hand, because of the EDX spectra of all membranes, sulfur atoms, especially in the PETMP cross-linker, were observed in all membranes by surface analysis. In addition, specific atoms of other counter ions such as B, P, and Cl were also detected in the membrane surface scan (See Supplementary Figure S6).

Furthermore, Table 1 presents the comparative swelling, water retention, and ion conductivity of pristine PVDF/PVP (M) and M_ALV-X-based membranes. Water absorption and swelling are different outcomes. Since water absorption in the membranes enhances ion transfer, it is a desirable property. As shown in Table 1, the addition of ALV-X-based materials increased both the water absorption rate and swelling values. Unlike water absorption, maintaining low values is crucial, as excessive swelling disrupts the membrane's bond structure, leading to mechanical instability. The PVDF membrane, known for its high chemical resistance, showed swelling rates similar to the Nafion membrane, even with the addition of ALV-X. The quantity of ion groups within a material is indicated by its ion exchange capacity (IEC), which is a critical factor of conductivity and, consequently, the transport properties of the membranes (Berezina et al., 2008). IEC of the membranes increased significantly with the addition of ALV-X. While the IEC of the pure PVDF membrane was 0.59 mmol g^{-1}, this value increased more than threefold to 0.86 mmol g^{-1} at M_ALV-PF_6^-. With the addition of ALV-ClO_4^-, the IEC value reached 1.18 mmol g^{-1}. The proportional increase in water absorption supports the relationship between water absorption and ion (OH^-) transfer. The highest value was obtained with M-ALV-BF_4^-, resulting in an IEC of 1.32 mmol g^{-1}. Thus, all M-ALV-X-based membranes displayed higher IEC values compared to Nafion 117 tested under similar conditions, while the swelling and water retention values remained within acceptable limits (Sharma et al., 2021).

Besides, electrochemical impedance spectroscopy (EIS) revealed the charge transfer behavior between the components of ALV-X membranes due to counterion exchange (Figure 4). Since the photochromic behavior of ALV-X depends on the mobility of counterions, high ionic conductivity is desired to achieve an excellent photochromic effect. The highest conductivity values, resulting from low resistance, were observed in M_ALV-ClO_4^- and ALV-BF_4^-, respectively. M_ALV-PF_6^- exhibited lower mobility due to its relatively larger ionic radius and showed higher resistance according to impedance measurements. Compared to the conventional Nafion 117 membrane (Neves et al., 2010), all viologen-based ALV-X membranes were exhibited high ionic conductivity (Table 2).

The photochromic effect of the membranes was achieved by applying a 366 nm UV lamp (30 W) to the surface and scanning the UV-Vis transmittance spectrum between 300 and 1,100 nm in 10-second intervals. Before the light exposure, it was determined that all membranes were more than 50% transmissive in the visible region, despite their light brown color. It was observed that the color of the membranes changed from light brown to dark green as the transmissive in the visible region decreased due to the bands centered at 610 nm and the shoulder bands at 575 nm, 670 nm, and 740 nm, which formed over time with the exposure of 366 nm. Additionally, according to the kinetic measurements taken at 610 nm under 366 nm, the transmittance of M_ALV-BF_4^- decreased from 49.6% to 4.8% in approximately 380 s. For M_ALV-ClO_4^-, the 610 nm transmittance decreased from 44.6% to 6.7% in 1,000 s. In the case of M_ALV-PF_6^-, this change occurred from 60% to 22.4% in approximately 1,800 s. The faster transmittance changes and also color turning response times in M_ALV-BF_4^- and M_ALV-ClO_4^- compared to M_ALV-PF_6^- may be attributed to the better ion mobility of BF_4^- and ClO_4^- as counterions compared to the larger ion PF_6^-. Moreover, as seen from the AFM images, the more uniform particle distribution of M-ALV-BF_4^- and M-ALV-ClO_4^- when compared to the M-ALV-PF_6^- may also be effective for the response time. In addition, after the membranes reached color saturation, the 366 nm UV light was turned off and the bleaching time was determined under room conditions. After 5,000 s, while the transmittance of M_ALV-BF_4^- at 610 nm increased from 4.8% to 9.2%, this value increased from 6.7 to 17.2 for ALV-ClO_4^-, and from 22.4% to 35.7% for M-ALV-PF_6^-, respectively (Figure 5). While a long time of approximately 12.5 h was required for M_ALV-BF_4^- for the color to fully return and the membranes to return to their previous state, it was measured that approximately 7 and 3 h were required for M_ALV-ClO_4^- and M_ALV-PF_6^-, respectively (See Supplementary Figures S7–S8). In addition, as a result of 10 consecutive scans, it was determined that the optical behaviors of M_ALV-BF_4^-, M_ALV-ClO_4^-, M_ALV-PF_6^- were preserved by 81%, 89% and 96%, respectively (See Supplementary Figure S9).

Figure 6 shows the color change of M_ALV-X membranes due to the transmittance change observed over 10 min under natural sunlight. Consistent with laboratory measurements conducted under 366 nm light, M_ALV-BF_4^- and M_ALV-ClO_4^- exhibited a more intense color change in the UV and visible regions compared to M_ALV-PF_6^-.

The chromic mechanism of viologens is based on a redox reaction that causes a color change when exposed to energy (i.e., voltage or light, etc.,) (Li et al., 2024; Wu et al., 2024). Viologens, typically 1,1′-disubstituted-4,4′-bipyridinium salts, have initially no absoption band at the visible range thus they are colorless (Monk et al., 2013). Upon light exposure, they undergo reduction, where they accept an electron and form a radical cation, which is colored. This process can occur due to the electron gaining energy

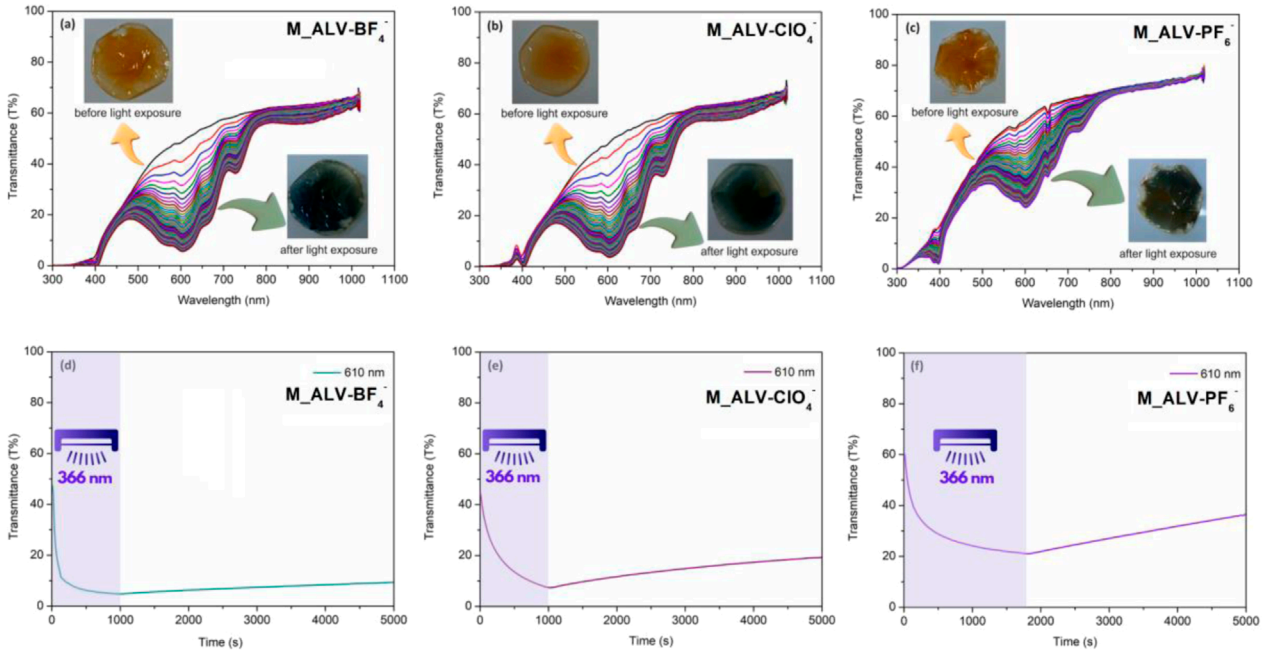

FIGURE 5
UV-Vis transmittance changes of M_ALV-BF_4^- **(A)**, M_ALV-ClO_4^- **(B)**, M_ALV-PF_6^- **(C)** and color changes kinetics of M_ALV-BF_4^- **(D)**, M_ALV-ClO_4^- **(E)**, M_ALV-PF_6^- **(F)** with and without light exposure.

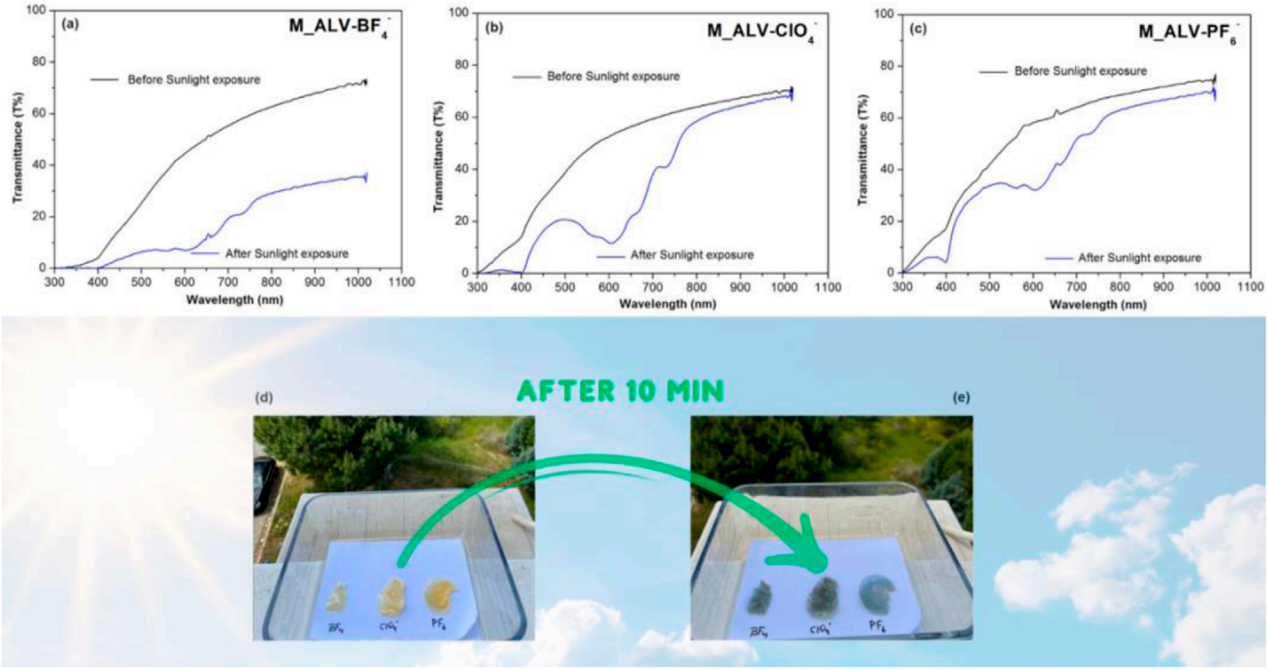

FIGURE 6
UV-Vis transmittance changes of M_ALV-BF_4^- **(A)**, M_ALV-ClO_4^- **(B)**, M_ALV-PF_6^- **(C)**, and color changes after 10 min under natural sunlight **(D,E)**.

from UV or visible light. The resulting radical cation should be stable in membrane and exhibits a distinct color change due to altered electron transitions (Striepe and Baumgartner, 2017). When the light source is removed, the viologen radical cation is oxidized back to its original colorless form, completing the reversible redox cycle. As a result, ALV-X based membranes exhibit photochromic

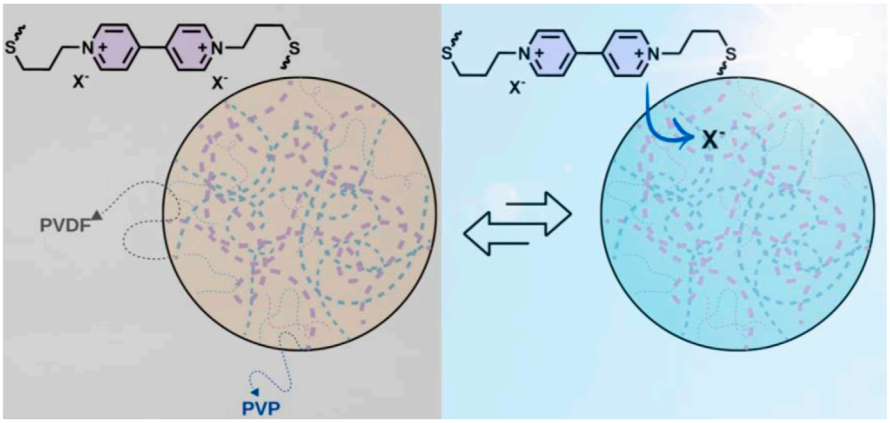

FIGURE 7
Proposed photochromic mechanism of M_ALV-X membranes.

effects as a result of the movements of counter ions with an external light source (Figure 7).

3 Conclusion

This study effectively demonstrates the photochromic properties of PVDF/PVP-based membranes doped with cross-linkable viologens with various counter anions ($-BF_4^-$, $-ClO_4^-$, or $-PF_6^-$). The membranes exhibit enhanced morphology and ion exchange ability. The porous structure increases the surface area, advantageous for multiple applications. They nearly completely block UV and visible light post-irradiation and show color changes under natural sunlight, consistent with lab observations. M-ALV-BF_4^- and M-ALV-ClO_4^- displayed faster and more intense color changes than M-ALV-PF_6^-, attributed to better ion mobility. These findings highlight the potential of M_ALV-X membranes as energy-saving coatings. This research provides valuable insights for developing high-performance, cost-effective alternative membranes, advancing materials science, and smart energy-saving technologies.

Data availability statement

The original contributions presented in the study are included in the article/Supplementary Material, further inquiries can be directed to the corresponding author.

Author contributions

JT: Formal Analysis, Investigation, Methodology, Resources, Software, Writing–original draft. SA: Conceptualization, Investigation, Software, Validation, Writing–original draft. MA: Formal Analysis, Investigation, Methodology, Writing–original draft. FU: Conceptualization, Data curation, Investigation, Methodology, Resources, Supervision, Validation, Writing–original draft. SK: Funding acquisition, Methodology, Project administration, Supervision, Validation, Writing–original draft, Writing–review and editing.

Funding

The author(s) declare that financial support was received for the research, authorship, and/or publication of this article. The author(s) declare financial support was received for the research, authorship, and/or publication of this article. This work was supported by the Office of Scientific Research Projects Coordination at Çanakkale Onsekiz Mart University (Grant number: FHD-2022-3899).

Conflict of interest

The authors declare that the research was conducted in the absence of any commercial or financial relationships that could be construed as a potential conflict of interest.

Publisher's note

Supplementary material

The Supplementary Material for this article can be found online at: https://www.frontiersin.org/articles/10.3389/fmats.2024.1490273/full#supplementary-material

References

Ambrose, B., Nasrin, K., Arunkumar, M., Kannan, A., Sathish, M., and Kathiresan, M. (2023). Viologen-based covalent organic polymers: variation of morphology and evaluation of their ultra-long cycle supercapacitor performance. *J. Energy Storage* 61, 106714. doi:10.1016/j.est.2023.106714

Berezina, N. P., Kononenko, N. A., Dyomina, O. A., and Gnusin, N. P. (2008). Characterization of ion-exchange membrane materials: properties vs structure. *Adv. Colloid Interface Sci.* 139, 3–28. doi:10.1016/j.cis.2008.01.002

Bhatti, I. N., Banerjee, M., and Bhatti, I. N. (2013). Effect of annealing and time of crystallization on structural and optical properties of PVDF thin film using acetone as solvent. *Iosr-Jap* 4, 42–47. doi:10.9790/4861-0444247

Chen, W., Shen, H., Zhu, X., Xing, Z., and Zhang, S. (2015a). Effect of citric acid on structure and photochromic properties of WO3–TiO2–ZnO composite films prepared by a sol–gel method. *Ceram. Int.* 41, 12638–12643. doi:10.1016/j.ceramint.2015.06.093

Chen, W., Shen, H., Zhu, X., Yao, H., and Wang, W. (2015b). Preparation and photochromic properties of PEG-400 assisted WO_3–TiO_2–ZnO composite films. *Ceram. Int.* 41, 14008–14012. doi:10.1016/j.ceramint.2015.07.013

Dallaev, R., Pisarenko, T., Sobola, D., Orudzhev, F., Ramazanov, S., and Trčka, T. (2022). Brief review of PVDF properties and applications potential. *Polymers* 14, 4793. doi:10.3390/polym14224793

Davis, A. R., and Carter, K. R. (2014). Surface grafting of vinyl-functionalized poly(fluorene)s via thiol–ene click chemistry. *Langmuir* 30, 4427–4433. doi:10.1021/la5000588

Davis, A. R., and Carter, K. R. (2015). Controlling optoelectronic behavior in poly(fluorene) networks using thiol–ene photo-click chemistry. *Macromolecules* 48, 1711–1722. doi:10.1021/ma5014226

Davis, A. R., Maegerlein, J. A., and Carter, K. R. (2011). Electroluminescent networks via photo "click" chemistry. *J. Am. Chem. Soc.* 133, 20546–20551. doi:10.1021/ja2088579

Du, J., Yang, Z., Lin, H., and Poelman, D. (2024). Inorganic photochromic materials: recent advances, mechanism, and emerging applications. *Responsive Mater.* 2, e20240004. doi:10.1002/rpm.20240004

Duncan, R. C., Faughnan, B. W., and Phillips, W. (1970). Photochromics and cathodochromics inorganic photochromic and cathodochromic recording materials. *Appl. Opt.* 9, 2236–2243. doi:10.1364/ao.9.002236

Hoyle, C. E., and Bowman, C. N. (2010). Thiol–ene click chemistry. *Angew. Chem. Int. Ed.* 49, 1540–1573. doi:10.1002/anie.200903924

Javed, H., Fatima, K., Akhter, Z., Nadeem, M. A., Siddiq, M., and Iqbal, A. (2016). Fluorescence modulation of cadmium sulfide quantum dots by azobenzene photochromic switches. *Proc. R. Soc. A Math. Phys. Eng. Sci.* 472, 20150692. doi:10.1098/rspa.2015.0692

Ju, G., Hu, Y., Chen, L., and Wang, X. (2013). Photochromism of rare earth doped barium haloapatite. *J. Photochem. Photobiol. A Chem.* 251, 100–105. doi:10.1016/j.jphotochem.2012.10.021

Kaiser, C., Halbritter, T., Heckel, A., and Wachtveitl, J. (2017). Thermal, photochromic and dynamic properties of water-soluble spiropyrans. *ChemistrySelect* 2, 4111–4123. doi:10.1002/slct.201700868

Kan, W.-Q., Wen, S.-Z., He, Y.-C., and Xu, C.-Y. (2017). Viologen-based photochromic coordination polymers for inkless and erasable prints. *Inorg. Chem.* 56, 14926–14935. doi:10.1021/acs.inorgchem.7b02206

Kayani, A. B. A., Kuriakose, S., Monshipouri, M., Khalid, F. A., Walia, S., Sriram, S., et al. (2021). UV photochromism in transition metal oxides and hybrid materials. *Small* 17, 2100621. doi:10.1002/smll.202100621

Koyuncu, S., and Ayaşlıgil, Ş. (2023). Synthesis and characterization of cross-linkable viologen derivatives. *J. Adv. Res. Nat. Appl. Sci.* 9, 615–623. doi:10.28979/jarnas.1267768

Kozlov, D. A., Shcherbakov, A. B., Kozlova, T. O., Angelov, B., Kopitsa, G. P., Garshev, A. V., et al. (2019). Photochromic and photocatalytic properties of ultra-small PVP-stabilized WO_3 nanoparticles. *Molecules* 25, 154. doi:10.3390/molecules25010154

Lee, J.-E., Eom, Y., Shin, Y.-E., Hwang, S.-H., Ko, H.-H., and Chae, H. G. (2019). Effect of interfacial interaction on the conformational variation of poly(vinylidene fluoride) (PVDF) chains in PVDF/graphene oxide (GO) nanocomposite fibers and corresponding mechanical properties. *Acs Appl. Mater. and Interfaces* 11, 13665–13675. doi:10.1021/acsami.8b22586

Li, C., Yang, W., Wang, M., Yu, X., Fan, J., Xiong, Y., et al. (2020). A review of coating materials used to improve the performance of optical fiber sensors. *Sensors* 20, 4215. doi:10.3390/s20154215

Li, L., Li, S.-H., Li, Z.-Y., Zhang, N.-N., Yu, Y.-T., Zeng, J.-G., et al. (2024). Advances in viologen-based stimulus-responsive crystalline hybrid materials. *Coord. Chem. Rev.* 518, 216064. doi:10.1016/j.ccr.2024.216064

Li, Z., Joshi, M. K., Chen, J., Zhang, Z., Li, Z., and Fang, X. (2020). Mechanically compatible UV photodetectors based on electrospun free-standing Y^{3+}-doped TiO_2 nanofibrous membranes with enhanced flexibility. *Adv. Funct. Mater.* 30, 2005291. doi:10.1002/adfm.202005291

Liu, F., Hashim, N. A., Liu, Y., Abed, M. R. M., and Li, K. (2011). Progress in the production and modification of PVDF membranes. *J. Membr. Sci.* 375, 1–27. doi:10.1016/j.memsci.2011.03.014

Martin, K. L., Nyquist, Y., Burnett, E. K., Briseno, A. L., and Carter, K. R. (2016). Surface grafting of functionalized poly(thiophene)s using thiol–ene click chemistry for thin film stabilization. *Acs Appl. Mater. and Interfaces* 8, 30543–30551. doi:10.1021/acsami.6b08667

Michaelis, L. (1935). Semiquinones, the intermediate steps of reversible organic oxidation-reduction. *Chem. Rev.* 16, 243–286. doi:10.1021/cr60054a004

Monk, P. M., Rosseinsky, D. R., and Mortimer, R. J. (2013). Electrochromic materials and devices based on viologens. *Electrochromic Mater. devices*, 57–90. doi:10.1002/9783527679850.ch3

Neves, L. A., Benavente, J., Coelhoso, I. M., and Crespo, J. G. (2010). Design and characterisation of Nafion membranes with incorporated ionic liquids cations. *J. Membr. Sci.* 347, 42–52. doi:10.1016/j.memsci.2009.10.004

Pathak, D. K., and Moon, H. C. (2022). Recent progress in electrochromic energy storage materials and devices: a minireview. *Mater. Horizons* 9, 2949–2975. doi:10.1039/d2mh00845a

Rajeevan, S., John, S., and George, S. C. (2021). Polyvinylidene fluoride: a multifunctional polymer in supercapacitor applications. *J. Power Sources* 504, 230037. doi:10.1016/j.jpowsour.2021.230037

Ru, Y., Shi, Z., Zhang, J., Wang, J., Chen, B., Huang, R., et al. (2021). Recent progress of photochromic materials towards photocontrollable devices. *Mater. Chem. Front.* 5, 7737–7758. doi:10.1039/d1qm00790d

Sen, S., Saraidaridis, J., Kim, S. Y., and Palmore, G. T. R. (2013). Viologens as charge carriers in a polymer-based battery anode. *ACS Appl. Mater. and Interfaces* 5, 7825–7830. doi:10.1021/am401590q

Sharma, G. D., Sharma, S., and Roy, M. S. (2003). Electrical and photoelectrical properties of dye-sensitized allyl viologen-doped polypyrrole solar cells. *Sol. Energy Mater. Sol. Cells* 80, 131–142. doi:10.1016/s0927-0248(03)00136-3

Sharma, P., Kumar, S., Bhushan, M., and Shahi, V. K. (2021). Ion selective redox active anion exchange membrane: improved performance of vanadium redox flow battery. *J. Membr. Sci.* 637, 119626. doi:10.1016/j.memsci.2021.119626

Shi, M. L., Liu, L., Tong, Y. J., Huang, L. K., Li, W. X., and Xing, W. H. (2019). Advanced porous polyphenylsulfone membrane with ultrahigh chemical stability and selectivity for vanadium flow batteries. *J. Appl. Polym. Sci.* 136. doi:10.1002/app.47752

Striepe, L., and Baumgartner, T. (2017). Viologens and their application as functional materials. *Chemistry–A Eur. J.* 23, 16924–16940. doi:10.1002/chem.201703348

Sun, M.-H., Huang, S.-Z., Chen, L.-H., Li, Y., Yang, X.-Y., Yuan, Z.-Y., et al. (2016). Applications of hierarchically structured porous materials from energy storage and conversion, catalysis, photocatalysis, adsorption, separation, and sensing to biomedicine. *Chem. Soc. Rev.* 45, 3479–3563. doi:10.1039/c6cs00135a

Tang, W., Zuo, C., Ma, C., Wang, Y., Li, Y., Yuan, X., et al. (2022). Designing photochromic materials with high photochromic contrast and large luminescence modulation for hand-rewritable information displays and dual-mode optical storage. *Chem. Eng. J.* 435, 134670. doi:10.1016/j.cej.2022.134670

Tian, H., and Zhang, J. (2016). *Photochromic materials: preparation, properties and applications*. Hoboken, NJ: John Wiley & Sons.

Tsuruoka, T., Hayakawa, R., Kobashi, K., Higashiguchi, K., Matsuda, K., and Wakayama, Y. (2016). Laser patterning of optically reconfigurable transistor channels in a photochromic diarylethene layer. *Nano Lett.* 16, 7474–7480. doi:10.1021/acs.nanolett.6b03162

Wang, M.-S., Xu, G., Zhang, Z., and Zheng, F.-K. (2010). Inorganic-organic hybrid photochromic materials. *Chem. Commun. Camb. Engl.* 46, 361–376. doi:10.1039/b917890b

Wu, L. Y. L., Zhao, Q., Huang, H., and Lim, R. J. (2017). Sol-gel based photochromic coating for solar responsive smart window. *Surf. Coatings Technol.* 320, 601–607. doi:10.1016/j.surfcoat.2016.10.074

Wu, W., Guo, S., Bian, J., He, X., Li, H., and Li, J. (2024). Viologen-based flexible electrochromic devices. *J. Energy Chem.* 93, 453–470. doi:10.1016/j.jechem.2024.02.027

Xu, G., Guo, G.-C., Wang, M.-S., Zhang, Z.-J., Chen, W.-T., and Huang, J.-S. (2007). Photochromism of a methyl viologen bismuth(III) chloride: structural variation before and after UV irradiation. *Angew. Chem. Int. Ed.* 46, 3249–3251. doi:10.1002/anie.200700122

Zhang, J., Zou, Q., and Tian, H. (2013). Photochromic materials: more than meets the eye. *Adv. Mater.* 25, 378–399. doi:10.1002/adma.201201521